

## Research Article

# Network Pharmacology and In Vivo Experimental Validation to Uncover the Renoprotective Mechanisms of Fangji Huangqi Decoction on Nephrotic Syndrome

Jiazhen Yin , Dongrong Yu , Lichan Mao , Caifeng Zhu , and Jin Yu 

Department of Nephrology,  
Hangzhou TCM Hospital Affiliated to Zhejiang Chinese Medical University (Hangzhou Hospital of Traditional Chinese Medicine), Hangzhou 310007, China

Correspondence should be addressed to Jin Yu; yujin8206@126.com

Received 7 May 2022; Accepted 20 May 2022; Published 8 June 2022

Academic Editor: Shuli Yang

Copyright © 2022 Jiazhen Yin et al. This is an open access article distributed under the Creative Commons Attribution License, which permits unrestricted use, distribution, and reproduction in any medium, provided the original work is properly cited.

**Background.** Fangji Huangqi decoction (FHD) is a traditional Chinese medicine formula that has the potential efficacy for nephrotic syndrome (NS) treatment. This study aims to explore the effects and underlying mechanisms of FHD against NS via network pharmacology and in vivo experiments. **Methods.** The bioactive compounds and targets of FHD were retrieved from the TCMSP database. NS-related targets were collected from GeneCards and DisGeNET databases. The compound-target and protein-protein interaction networks were constructed by Cytoscape 3.8 and BisoGenet, respectively. GO and KEGG analyses were performed by the DAVID online tool. The interactions between active compounds and hub genes were revealed by molecular docking. An NS rat model was established to validate the renoprotective effects and molecular mechanisms of FHD against NS in vivo. **Results.** A total of 32 hub genes were predicted to play essential roles in FHD treating NS. Eight main bioactive compounds of FHD had the good affinity with 9 hub targets (CCL2, IL-10, PTGS2, TNF, MAPK1, IL-6, CXCL8, TP53, and VEGFA). The therapeutic effect of FHD on NS was closely involved in the regulation of inflammation and PI3K-Akt pathway. In vivo experiments confirmed the renoprotective effect of FHD on NS, evidenced by reducing the levels of proteinuria, serum creatinine, blood urea nitrogen, and inflammatory factors in NS rats. The PI3K activator 740Y-P weakened the effects of FHD against NS. Furthermore, FHD downregulated the levels of PTGS2, MAPK1, IL-6, and p-Akt in NS rats. **Conclusions.** FHD alleviates kidney injury and inflammation in NS by targeting PTGS2, MAPK1, IL-6, and PI3K-Akt pathway.

## 1. Introduction

Nephrotic syndrome (NS) is a clinical syndrome commonly characterized by edema, hyperlipidemia, hypoalbuminemia, and heavy proteinuria [1]. The incidence of NS is caused by diverse reasons, including auto-antibodies to specific glomerular antigens, genetic mutations, infections, metabolic disorders, podocytopathies, or paraneoplastic syndromes [2]. NS is one of the most common types of chronic kidney disease diagnosed in clinic. It has been reported that the incidence of NS accounts for 40% of all the renal biopsies, in which primary NS accounts for 75% [3]. At present, the pathogenesis of NS is not clear, and the therapeutic

approaches are limited. As a consequence, there is an urgent need for a safer and more effective drug against NS.

Traditional Chinese medicines (TCMs) have attracted great attention for NS treatment, due to their favorable properties of low side effects, recurring rate, and cost [4]. Importantly, TCMs exert therapeutic effects by coordinating multicomponents and multitargets. Fangji Huangqi decoction (FHD), one of the classical TCMs formula, is composed of four medicinal herbs including *Stephania Tetrandra Radix* (Fangji, FJ), *Astragali Radix* (Huangqi, HQ), *Glycyrrhiza Radix* (Gancao, GC), and *Atractylodis Macrocephalae Rhizoma* (Baizhu, BZ). As the main herb in the FHD, FJ has been reported to possess various pharmacological

properties, such as immunomodulatory, anti-inflammatory, anticancer, antifibrotic, antiplatelet, and antidiabetic effects [5]. Similarly, HQ, GC, and BZ also have been demonstrated to exhibit commendable pharmacological activities, including immunomodulation, antioxidation, inhibition of liver fibrosis, cardiovascular protection, stimulation of blood regeneration, and pain-relieving properties [6–8]. However, potential mechanisms of FHD in the treatment of NS are still illusive.

TCMs are characterized by multicomponent and multitarget, which exert therapeutic effects on diverse diseases via bioactive components acting on multiple targets [9]. Network pharmacology, an emerging and promising subject, is a powerful tool to explore the associations between active components and potential targets for TCMs treating complex diseases [10]. Network pharmacology systematically studies the interaction between “drug-target-pathway-disease” based on the integration of bioinformatics, molecular biology, and public database information. Varghese and Majumdar proposed network pharmacology as an initial inherent approach in identifying the repurposing and synergism of drug candidates for NS treatment [11]. Some previous studies have identified the efficacy and underlying mechanisms of TCMs treating NS via network pharmacology [12, 13]. For instance, Yiqi Huoxue Decoction has been found to enhance renal function and alleviate podocyte injury in NS, and the potential mechanisms involved PI3K-AKT and NF- $\kappa$ B pathways based on network pharmacology [12]. Duan et al. established the underlying mechanism of Qingreka-sen granule against NS, including promoting autophagy and antiapoptosis through regulating the expression of AKT1, CASP3, BCL2L1, and mTOR to protect podocytes and maintain renal tubular function [13]. Furthermore, Zhang et al. revealed that FHD possesses the antinephrotic syndrome effect in rat nephropathy model; however, the relative underlying mechanisms have not been fully elucidated [14]. In this study, a systematic network pharmacology approach was applied to predict the bioactive components and hub targets for FHD against NS. Moreover, *in vivo* experiments were performed to validate the therapeutic efficacy of FHD on NS, and the potential mechanism (PI3K-Akt pathway) and hub targets [prostaglandin-endoperoxide synthase 2 (PTGS2), mitogen-activated protein kinase 1 (MAPK1), and interleukin 6 (IL-6)] were uncovered. Also, a total of 144 bioactive compounds of FHD and 62 overlapping targets of FHD against NS were discovered for further investigation. This study provides a potential therapeutic drug for NS and offers the essential foundation for the mechanism investigation of FHD treating NS.

## 2. Materials and Methods

### 2.1. Screening of Bioactive Compounds and Targets of FHD.

The active compounds and targets of FHD were retrieved from the TCM systems pharmacology (TCMSP) analysis platform (<https://tcmssp.com/tcmssp.php>). All potential active compounds were subjected to absorption,

distribution, metabolism, and excretion (ADME) of drugs screened with the criteria of oral bioavailability (OB)  $\geq$  30% and drug-likeness (DL)  $\geq$  0.18 [15]. Besides, bioactive compounds with targets  $>$ 3 were also selected as candidates. More active components of FHD with significant pharmacological effects were supplemented based on previous literature. Subsequently, target proteins of active compounds were predicted in SwissTargetPrediction database (<https://www.swisstargetprediction.ch/>) with the criteria of probability  $>$ 0.5.

**2.2. Construction of Herb-Compound-Target (H-C-T) Network.** Active compounds of FHD and their corresponding targets were subjected to establish the H-C-T network. H-C-T network was constructed by Cytoscape (version 3.8, <https://www.cytoscape.org/>), an open software package project for visualizing, integrating, modeling, and analyzing the interaction network [16].

**2.3. Screening of NS-Related Targets.** The therapeutic targets for NS were obtained from GeneCards database (<https://www.genecards.org>) [17] and DisGeNET database (<https://www.disgenet.org/>) [18]. The words “minimal change disease,” “membranous nephropathy,” “focal segmental glomerulosclerosis,” “mesangial proliferative glomerulonephritis,” and “mesangial capillary glomerulonephritis” were used as index words, and the species were limited to “*Homo sapiens*” in the collection of therapeutic targets. The targets belonging to both databases were retained as candidate targets. STRING database (<https://string-db.org/>) was applied to construct the NS targets network based on the candidate NS-related therapeutic targets [19].

**2.4. Construction of Protein-Protein Interaction (PPI) Network.** The overlapping targets of disease and drug component were mapped with Venn diagram by online tools (<https://bioinformatics.psb.ugent.be/webtools/Venn/>) for further analysis. The Cytoscape plugin BisoGenet was conducted for the construction of PPI network for overlapping targets. The PPI network was thereafter inputted into Cytoscape for visualization. The PPI network was analyzed by Cytoscape plugin CytoHubba, and the hub genes were screened with the criteria of degree more than twice the median.

**2.5. Gene Ontology (GO) and Kyoto Encyclopedia of Genes and Genome (KEGG) Pathway Enrichment Analyses.** The Database for Annotation, Visualization and Integrated Discovery (DAVID, <https://david.ncicrf.gov/>) was used to perform GO and KEGG pathway enrichment analyses with  $P < 0.05$ . The enriched GO and KEGG pathway terms were visualized by the Matplotlib [20].

**2.6. Molecular Docking.** The 2D structure of the eight core compounds were downloaded from Zinc 15 [21]. The compound’s structures were added into AutoDockTools (version 1.5.6) [22] to add polar hydrogen, distribute charge,

set rotatable keys, and save as “PDBQT” file. The 3D structures of the top nine hub genes were downloaded from the Protein Data Bank (PDB) database [23]. Separation of the target proteins from the original ligand and removal of water molecules was performed using PyMOL (version 2.3.0) [24]. The ligand and receptor were imported into AutoDockTools (version 1.5.6) to add polar hydrogen, distribute charge, and save as “PDBQT” file. Molecular docking was performed using AutoDock Vina (version 1.1.2) [25], and interaction pattern analysis was carried out using PyMOL to map combinations with the lowest binding energy (affinity).

### 2.7. *In Vivo* Experimental Validation

**2.7.1. Experimental Animals and Drug Treatment.** All animal experiments were approved by the Institutional Animal Care and Use Committee and the local experimental ethics committee. Male Sprague-Dawley (SD) rats ( $n = 36$ ) were purchased from Shanghai SLAC Laboratory Animal Co., Ltd. (Shanghai, China). Rats were kept under a 12 h light/dark cycle with  $45 \pm 15\%$  humidity at  $23 \pm 1^\circ\text{C}$  and had free access to food and water. After one week, SD rats were randomly divided into six groups ( $n = 6$  per group): the control group (no treatment); the model group; the low-FHD group; the mid-FHD group; the high-FHD group; and the FHD + 740Y-P group. In order to induce NS, rats in the model and drug-treated groups were intravenously injected with 4 mg/kg adriamycin (ADR) and then injected with 1 mg/kg ADR after one week. Rats in the control group were intravenously injected with saline. After modeling, NS rats in the low-, mid-, and high-FHD groups were, respectively, administrated with 1, 2, and 4 g/kg/d FHD by oral gavage for 30 days. NS rats in the FHD + 740Y-P group were gavaged with 4 g/kg/d FHD and intraperitoneally injected with 20  $\mu\text{M}$  740Y-P (a PI3K activator). Rats in the control and model group received equal volumes of water. The body weights of rats were recorded once every 4 weeks. After treatment, 24 h urines of all rats were collected to measure the level of urine protein using a BCA kit (Thermo Fisher Scientific, IL, USA). At the end point of treatment, all rats were anesthetized with 10% sodium pentobarbital and blood samples were collected via retro-orbital puncture. Rats were sacrificed by cervical dislocation and right kidneys were removed and weighed to calculate the kidney index (kidney weight/body weight).

**2.8. Measurement of Inflammatory Factors and Renal Function Indicators.** Blood samples were collected from orbits of rats and the serum was separated via centrifuging for 20 min at 3,000 r/min. The levels of serum inflammatory factors (IL- $\beta$ , MCP-1, and TGF- $\beta$ 1) were measured by the corresponding enzyme-linked immune-sorbent assay (ELISA) kits (Mlbio, China). For the assessment of renal function, the levels of serum creatinine (SCr), blood urea nitrogen (BUN), and albumin (ALB) were determined using a chemical analyzer (Fujifilm, Japan).

**2.9. Hematoxylin and Eosin (H&E) Staining.** Right kidneys of rats were removed and fixed in 4% formaldehyde for 24 h. Next, kidney tissues were dehydrated in alcohol and then embedded in paraffin. Tissues were sliced into 4  $\mu\text{m}$ -thick sections and went through dewaxing and hydration. Followed by that, sections were stained with hematoxylin for 5 min and with eosin for 2 min. The renal pathological changes were observed under a light microscope (Olympus, Japan).

**2.10. qRT-PCR.** Total RNA of kidney tissues was extracted using TRIzol reagent (Invitrogen, CA, USA) and were reversely transcribed to cDNA using the PrimeScript One-Step RT-PCR Kit (Takara, Japan). qRT-PCR was performed using the SYBR Green qPCR master Mix kit and the Agilent Stratagene Mx3000P Real-Time PCR instrument (DBI Bioscience, China). Reaction program was  $95^\circ\text{C}$  for 3 min, and 40 cycles of  $95^\circ\text{C}$  for 12 s and  $62^\circ\text{C}$  for 40 s. The primers used in this work were listed in Table S1. The relative mRNA expression of target genes was calculated using the  $2^{-\Delta\Delta\text{Ct}}$  method by normalizing to GAPDH.

**2.11. Western Blot Analysis.** Total protein was extracted from kidney tissues using the lysis buffer (Beyotime, China) and quantified using the BCA kit (Thermo Fisher Scientific, MA, USA). Proteins were separated on 10% SDS-PAGE and then transferred onto polyvinylidene fluoride membranes (Millipore, MA, USA). After blocking with 5% skim milk for 1 h, membranes were incubated with primary antibodies at  $4^\circ\text{C}$  overnight. Then, membranes were incubated with horseradish peroxidase (HRP)-conjugated secondary antibodies for 1 h under dark condition. Protein bands were visualized using the ECL Substrate Kit (Abcam, UK) and photographed under the ChemiDoc Imaging System (Bio-Rad, CA, USA). The primary antibodies used in Western blotting were rabbit monoclonal anti-PTGS2 (1 : 1,000; GST, MA, USA), mouse monoclonal anti-IL-6 (1 : 500; Abcam, UK), rabbit monoclonal anti-MAPK1 (1 : 2,000; GST), rabbit polyclonal anti-Akt (1 : 1,000; Abcam), rabbit polyclonal anti-p-Akt (1 : 500; Abcam), and mouse monoclonal anti-GAPDH (1 : 500; Abcam). The secondary antibodies were rabbit anti-mouse IgG H&L and goat anti-rabbit IgG H&L (1 : 2,000; Abcam).

**2.12. Statistical Analysis.** All data were processed on the GraphPad 7.0 and presented as mean  $\pm$  standard deviation. The comparison between groups was analyzed using the one-way ANOVA, followed by Tukey’s test.  $P < 0.05$  was taken as the measure of statistical difference.

## 3. Results

**3.1. H-C-T Network of FHD.** According to the public database and previous literature, a total of 114 bioactive compounds of FHD were collected (Table S2). There were 11 active compounds from *Stephaniae Tetrandrae Radix* (FJ), 16 from *Astragali Radix* (HQ), 6 from *Atractylodes macrocephalae Rhizoma* (BZ), and 81 from *Liquiritiae Radix* et

Rhizoma (GC). Subsequently, a total of 552 targets of these bioactive compounds were obtained from SwissTargetPrediction database. A H-C-T network was constructed to visualize the interactions between compounds and targets of FHD. This H-C-T network included 670 nodes (4 herbs, 114 compounds, and 552 targets) and 2781 edges (interactions between two target proteins) with an average degree of 8.418 (Figure 1).

### 3.2. Identification of Overlapping Targets for FHD Against NS.

Based on the public databases, 302 NS-related targets were obtained and a PPI network of these targets was constructed. The PPI network of NS-related targets included 297 nodes and 4361 edges with an average degree of 29.4 (Figure 2). In addition, a Venn diagram showed that there were 62 overlapping targets obtained by comparing the targets of FHD and NS, which were deemed to be potential therapeutic targets of FHD against NS (Figure 3(a)). The interactions among 62 overlapping targets were visualized by a PPI network. As shown in Figure 3(b), the PPI network of overlapping targets included 62 nodes and 749 edges with an average degree of 22.4. The top 25 hub targets were screened including INS, TNF, VEGFA, IL6, TP53, IL1B, PTGS2, CXCL8, HIF1A, ESR1, CCL2, IL10, TLR4, EDN1, ACE, IL4, TGFB1, APOE, LEP, NOS3, SPP1, SERPINE1, MAPK1, CCND1, and KDR (Figure 3(b)).

### 3.3. GO and KEGG Pathway Enrichment Analysis.

DAVID was applied for the GO enrichment and KEGG pathway enrichment of the 62 hub targets. The results of GO enrichment analysis indicated that 67 biological processes (BP), 4 cellular components (CC), and 10 molecular functions (MF) were obtained. In the BP ontology, the targets of the PPI network primarily associated with positive regulation of nitric oxide biosynthetic process, lipopolysaccharide-mediated signaling pathway, positive regulation of transcription from RNA polymerase II promoter, cellular response to lipopolysaccharide, angiogenesis, inflammatory response, positive regulation of NF- $\kappa$ B transcription factor activity, and positive regulation of sequence-specific DNA binding transcription factor activity (Figure 4(a)). For the CC ontology, the targets located mainly in extracellular space, extracellular region, external side of plasma membrane, platelet alpha granule lumen, caveola, secretory granule, extracellular matrix, blood microparticle, and protein complex (Figure 4(b)). Based on GO annotation of MF, it could be seen that the targets were mainly involved in cytokine activity, growth factor activity, enzyme binding, transcription factor binding, hormone activity, heparin binding, and transcriptional activator activity (Figure 4(c)).

The results of KEGG pathway enrichment revealed that the hub targets mainly related to HIF-1 signaling pathway, NOD-like receptor signaling pathway, proteoglycans in cancer, PI3K-Akt signaling pathway, Toll-like receptor signaling pathway, and TNF signaling pathway (Figure 5). The top 30 GO terms and top 20 KEGG

pathways of hub targets were, respectively, shown in Tables S3 and S4.

### 3.4. Molecular Docking of Core Compounds and Hub Genes.

The binding affinity between core compounds and hub genes of FHD were verified by molecular docking. As shown in Table 1, the eight bioactive compounds were palmatine,  $\beta$ -elemene, tetrandrine, fangchinoline, bifendate, calycosin, atractylenolide I, hinesol. The 9 hub targets were CCL2, IL10, PTGS2, TNF, MAPK1, IL6, CXCL8, TP53, and VEGFA. AutoDock Vina assessed the binding strength of small molecules and proteins primarily through affinity. A threshold affinity  $< -5$  kcal/mol was set in this study. A total of 58 docking pairs were obtained as shown in Table S5. Tetrandrine showed the high binding affinity of  $-10.1$  kcal/mol with TNF and  $-8.6$  kcal/mol with IL10. Fangchinoline showed the high binding affinity of  $-9.5$  kcal/mol with IL-10 and  $-9.5$  kcal/mol with TNF. Palmatine showed the high binding affinity of  $-8.6$  kcal/mol with TNF and  $-8.5$  kcal/mol with CCL2. Calycosin showed the high binding affinity of  $-8.6$  kcal/mol with PTGS2,  $-8.5$  kcal/mol with TNF,  $-8.3$  kcal/mol with TP53, and  $-8.2$  kcal/mol with CCL2. The small-molecule compounds were tightly bound to the protein residues via various interactions (Figure 6).

### 3.5. In Vivo Experimental Validation

#### 3.5.1. Effects of FHD on Body Weight, Kidney Weight, Proteinuria, and Inflammatory Response in NS Rats via Affecting PI3K-Akt Signaling Pathway.

The therapeutic effect and mechanism of FHD on NS were next validated in NS rats induced by ADR. As depicted in Figure 7(a), NS rats showed evident loss of body weight when compared with control rats ( $P < 0.05$ ). After administration of high-dose FHD, the body weight of NS rats was significantly increased ( $P < 0.05$ ; Figure 7(a)). The increase of kidney weight is an important indicator of kidney tissue damage [26]. In this study, the right kidney index of NS rats markedly increased versus control rats, which was dose-dependently prevented by treating with FHD ( $P < 0.001$ ; Figure 7(b)). Proteinuria is also a critical biomarker for diverse renal diseases. In this work, the 24 h urines of rats after 4-week drug administration were collected and the level of urine protein was determined. As expected, NS rats presented severe proteinuria as evidenced by the remarkable increase in the excretion of urine protein compared with control rats ( $P < 0.001$ ). The administration of FHD markedly reduced the level of urine protein in NS rats ( $P < 0.001$ ; Figure 7(c)). Moreover, inflammatory response in kidney is an important characteristic of NS, and IL-1 $\beta$ , MCP-1, and TGF- $\beta$ 1 are critical proinflammatory cytokines [27]. ELISA showed that the levels of serum IL-1 $\beta$ , MCP-1, and TGF- $\beta$ 1 were significantly increased in NS rats, but FHD treatment attenuated the secretion of these inflammatory cytokines ( $P < 0.01$ ; Figures 7(d)–7(f)). In addition, several reports have indicated that PI3K-Akt signaling pathway acts as a pivotal role in kidney diseases [28–30]. Network pharmacological analysis also proved the essential role of PI3K-Akt

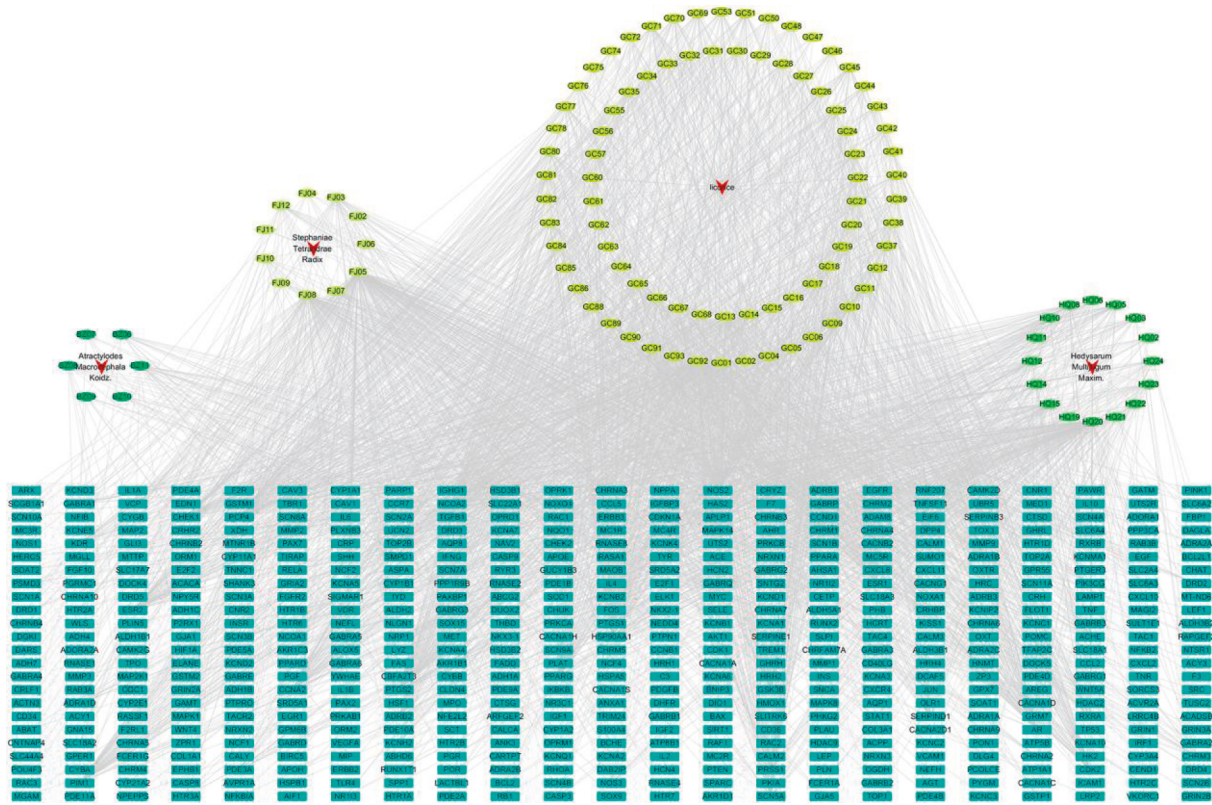


FIGURE 1: Herb-compound-target network of Fangji Huangqi decoction (FHD). Red arrows represent 4 herbs, green and yellow circles represent compounds, and blue rectangles represent targets.

pathway in FHD treating NS. In the present study, we found that 740Y-P (a PI3K activator) treatment significantly weakened the therapeutic effect of FHD on NS rats as indicated by the decreased body weight and the increased right kidney index, urine protein level, and inflammatory cytokines ( $P < 0.05$ ; Figures 7(a)–7(f)).

**3.5.2. Effects of FHD on Renal Function and Histopathological Changes in NS Rats via Affecting PI3K-Akt Signaling Pathway.** The therapeutic effects of FHD on renal function and histopathological changes induced by NS were further evaluated. SCr, BUN, and ALB are three critical indicators widely used to identify kidney function [31]. As shown in Figures 8(a)–8(c), the levels of SCr and BUN were significantly increased in serum of NS rats, and ALB level was decreased in comparison to that in control rats ( $P < 0.001$ ). FHD treatment markedly downregulated the abundance of SCr and BUN and upregulated the ALB level in NS rats in a dose-dependent manner, but the effects of FHD was weakened by 740Y-P addition ( $P < 0.05$ ; Figures 8(a)–8(c)). Additionally, compared with control rats, H&E staining exhibited the serious renal histological damage in NS rats with thickened glomerular basement membrane, hollow renal tubules, and glomerular and tubular atrophy. However, these histopathological indications were mitigated after FHD treatment, in particular high-dose FHD treatment, whereas 740Y-P addition weakened the effect of FHD (Figure 8(d)).

**3.6. Confirmation of Hub Targets for FHD Treating NS.** Based on the network pharmacological analysis, 9 hub targets (CCL2, IL10, PTGS2, TNF, MAPK1, IL6, CXCL8, TP53, and VEGFA) were collected and validated as the therapeutic targets of FHD on NS in vivo. qRT-PCR showed the increased CCL2 expression and the decreased VEGFA level in NS rats compared with that in control rats ( $P < 0.05$ ), and there were no significant changes after FHD or/and 740Y-P treatment (Figures 9(a) and 9(b)). The expression of PTGS2, MAPK1, and IL-6 was significantly upregulated in NS rats when compared to that in control rats, whereas IL-10 expression was downregulated ( $P < 0.001$ ). FHD treatment dose-dependently rescued the expression levels of PTGS2, MAPK1, IL-6, and IL-10 in NS rats, whereas 740Y-P addition weakened the effect of FHD ( $P < 0.05$ ; Figures 9(c)–9(f)). For the expression of TNF, CXCL8, and TP53, they were dramatically upregulated in NS rats in comparison to that in control rats ( $P < 0.001$ ). High-dose FHD treatment rescued the expression levels of TNF, CXCL8, and TP53 in NS rats, whereas 740Y-P addition weakened the effects of FHD ( $P < 0.001$ ; Figures 9(g)–9(i)). In addition, Western blotting confirmed the results of qRT-PCR on the expression of PTGS2, MAPK1, and IL-6 ( $P < 0.01$ ; Figures 10(a)–10(d)). Meanwhile, the protein level of p-AKT was increased in NS rats compared to that in control rats, which was rescued by FHD administration in a dose-dependent manner ( $P < 0.05$ ). Similarly, 740Y-P treatment weakened the

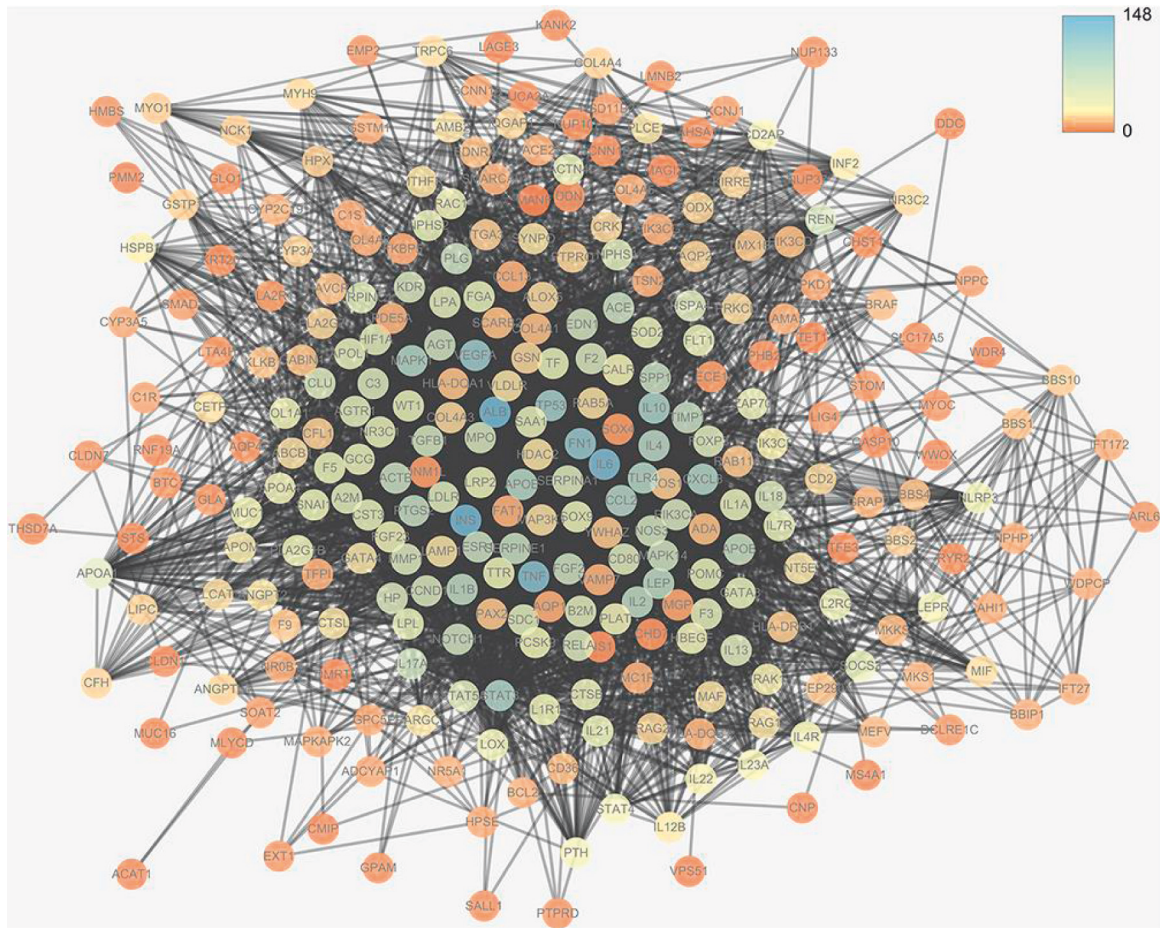


FIGURE 2: Protein-protein interaction (PPI) network of nephrotic syndrome- (NS-) related targets. Colors from orange to blue are proportional to the degrees of nodes.

inhibitory effect of FHD on p-AKT expression in NS rats ( $P < 0.001$ ; Figures 10(a), 10(e), and 10(f)).

#### 4. Discussion

NS is a highly prevalent kidney disease with the clinical triad of heavy proteinuria, edema, and hypoalbuminemia [2]. Currently, most therapeutics for NS mainly target the NS-related secondary symptoms, which cannot prevent the disease from further developing into renal failure [32]. Therefore, more effective NS treatment drugs and strategies still need to be further investigated. In recent years, TCMs are increasingly becoming the promising therapeutic drugs for kidney diseases for their low side effects and commendable pharmacological activities [33]. FHD is a classical TCMs firstly recorded in Synopsis of the Golden Chamber and widely used in the treatment of edema and dysuria [4]. In this study, based on network pharmacology and functional enrichment analyses, 9 hub targets (CCL2, IL-10, PTGS2, TNF, MAPK1, IL-6, CXCL8, TP53, and VEGFA) and PI3K-Akt pathway were predicted as the potential target mechanisms for FHD treating NS. Furthermore, *in vivo* experiments validated the therapeutic efficacy of FHD against NS and the potential mechanisms by targeting PI3K-Akt pathway, PTGS2, MAPK1, and IL-6.

Based on network pharmacological analysis, 8 main bioactive compounds (palmatine,  $\beta$ -elemene, tetrandrine, fangchinoline, bifendate, calycosin, atractylenolide I, and hinesol) of FHD were predicted to have good affinity with 9 hub targets (CCL2, IL-10, PTGS2, TNF, MAPK1, IL-6, CXCL8, TP53, and VEGFA) for NS treatment. It has been reported that CCL2, IL-10, PTGS2, TNF, IL-6, and CXCL8 were closely bound up with the pathogenic process of NS via regulating immunity and inflammation [34–38]. MAPK1 is a member of mitogen-activated protein kinases that are involved in the regulation of NS progression through activating downstream signals [39]. TP53 and VEGFA are also important molecules that act as important roles in renal microangiogenesis and maintain the functions of kidney [40, 41]. In addition, tetrandrine can reduce the levels of inflammatory factors TNF- $\alpha$  and IL-6 and elevate IL-10 level in rats with diabetic nephropathy (DN) [42]. Calycosin also can ameliorate diabetes-induced renal inflammation as indicated by the reduced TNF- $\alpha$  level [43]. Fangchinoline exhibits the nephroprotective effects in DN rats via attenuating inflammation and MAPK signaling pathway [44]. Molecular docking in this study further showed that these bioactive compounds of FHD interact with hub targets (CCL2, IL-10, PTGS2, TNF, MAPK1, IL-6, CXCL8, TP53,

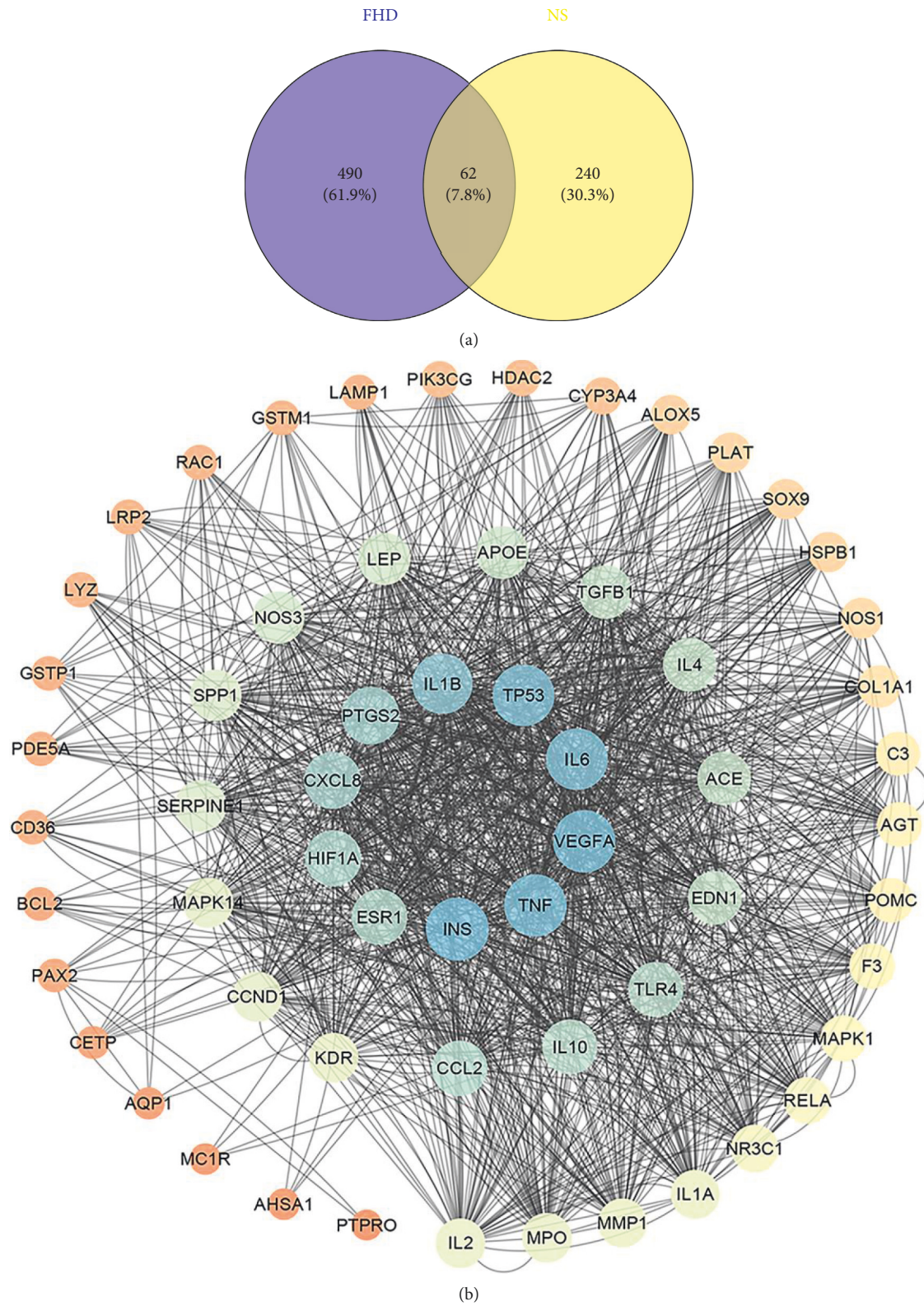


FIGURE 3: PPI network of potential therapeutic targets for FHD against NS. (a) Venn map of overlapping targets on FHD and NS. The purple circle indicates the targets of FHD, and the yellow circle indicates the targets of NS. The part of the two intersecting circles is the overlapping targets. (b) PPI network of overlapping targets on FHD and NS. Colors from orange to blue are proportional to the degrees of nodes.

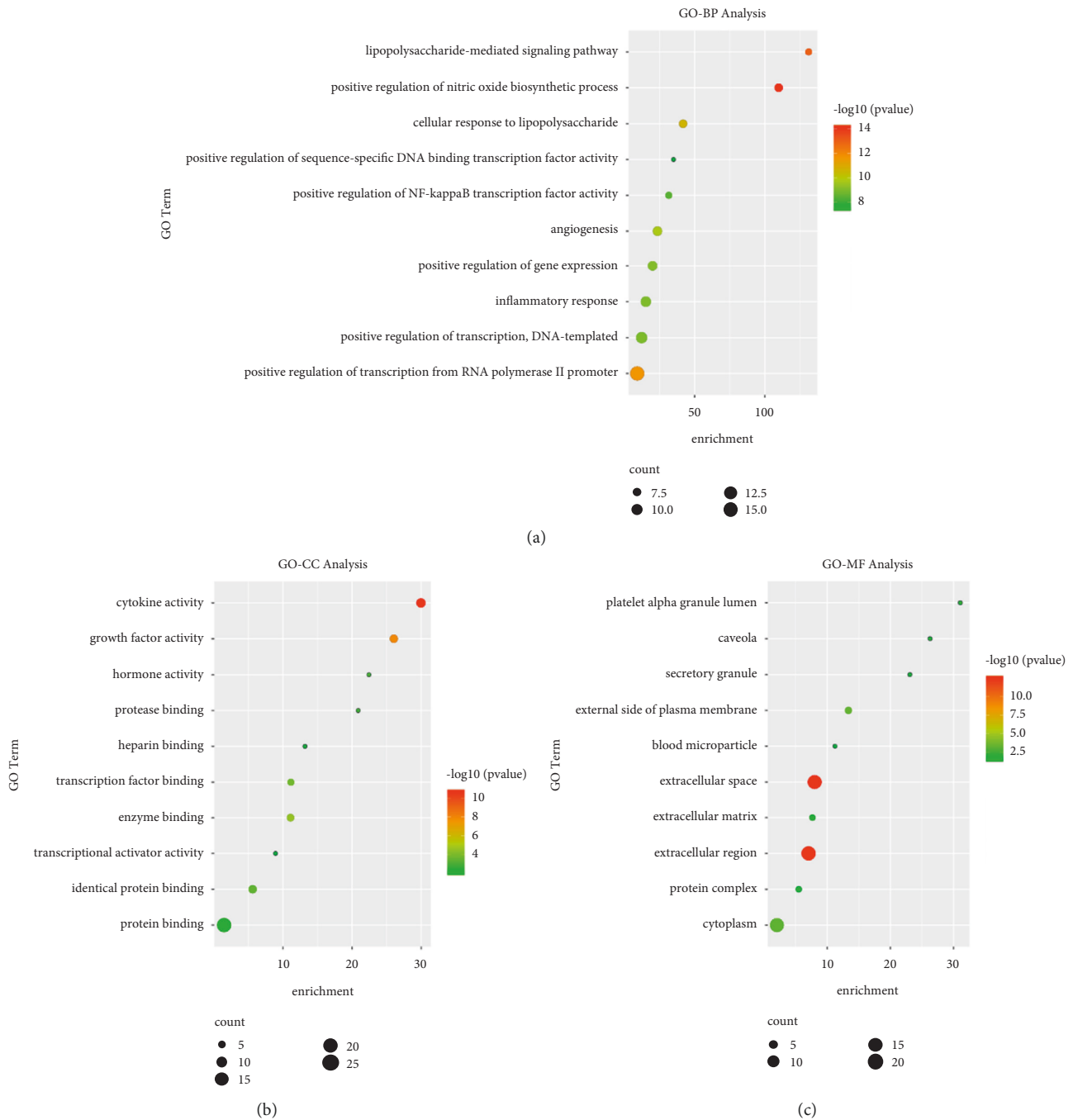


FIGURE 4: Gene ontology (GO) enrichment analysis for hub target genes of FHD treating NS. (a) The top 10 enriched terms in biological process (BP). (b) The top 10 enriched terms in cellular component (CC). (c) The top 10 enriched terms in molecular function (MF).

and VEGFA) with best affinity  $< -5$  kcal/mol. These results indicate that these 9 hub targets might play critical roles in the therapeutic effect of FHD against NS.

Furthermore, GO and KEGG pathway enrichment analyses were applied to further illustrate the mechanisms of FHD in NS treatment. The GO enrichment analysis showed that hub genes mainly function in the regulation of NF- $\kappa$ B transcription factor activity and inflammatory response. NF- $\kappa$ B transcription factor is an important regulator for cellular behaviors and immune activation, the inhibition of which

can protect against renal inflammation [45]. These further confirm that the therapeutic efficacy of FHD against NS is closely associated with immunoregulation. In KEGG pathway enrichment analysis, hub targets were mainly enriched in Toll-like receptor, NOD-like receptor, and PI3K-Akt signaling pathways. Accumulating evidence has indicated that PI3K-Akt pathway plays an indispensable role in the regulation of kidney diseases [28–30]. Tu Di et al. demonstrated that the inhibition of PI3K/Akt/mTOR pathway can alleviate renal oxidative stress in membranous



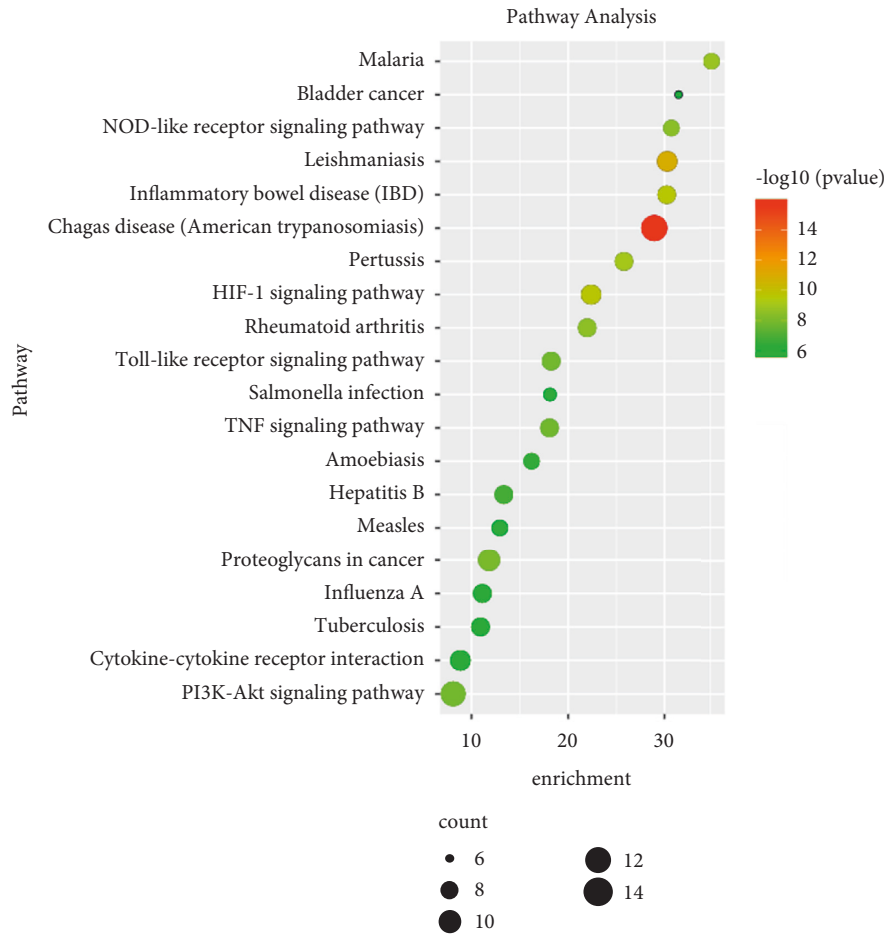


FIGURE 5: Kyoto Encyclopedia of Genes and Genomes (KEGG) pathway analysis for hub target genes of FHD treating NS. The color of circles represents the  $P$  value, and the size of circles represents the count.

nephropathy [28]. Yin et al. revealed that tetrandrine protects against membranous glomerulopathy through targeting PI3K-Akt signaling pathway [29]. Liu and He also elucidated that the suppression of PI3K-Akt pathway can alleviate the inflammatory response, thereby ameliorating focal segmental glomerulosclerosis [30]. Therefore, we considered that PI3K-Akt pathway plays an essential role in FHD treating NS.

To validate the molecular mechanisms predicted by network pharmacology and enrichment analyses, an NS rat model was established by ADR induction. The significantly decreased body weight, the increased kidney index, and the disordered pathophysiology were observed in NS rats, indicating that the establishment of NS rat model was successful. FHD dose-dependently inhibited the decreased body weight and the increased kidney index in NS rats, where 740Y-P (a PI3K activator) weakened the effects of FHD. These results preliminary proved the therapeutic efficacy of FHD against NS and revealed the mechanism involving in

PI3K-Akt pathway. Massive proteinuria is a typical clinical syndrome of NS, which was exhibited in NS rats. However, FHD treatment reduced the level of urine protein in NS, where 740Y-P weakened the effect of FHD. SCr, BUN, and ALB are critical assessment indicators for renal function, the levels of which in NS rats were reduced after FHD treatment. In addition, FHD reduced the levels of inflammatory factors (IL-1 $\beta$ , MCP-1, and TGF- $\beta$ 1) in NS rats. These results indicating that FHD can protect renal function and alleviate inflammation in NS. However, 740Y-P weakened the renoprotective effects of FHD in NS, suggesting that FHD treating NS is involved in the regulation of PI3K-Akt pathway. Furthermore, qRT-PCR and Western blot analyses showed that FHD dose-dependently downregulated the expression of PTGS2, MAPK1, IL-6, and p-Akt in NS. Combined with the results of network pharmacology, these discoveries indicate that FHD exerts the therapeutic effect on NS by targeting PTGS2, MAPK1, IL-6, and PI3K-Akt pathway.

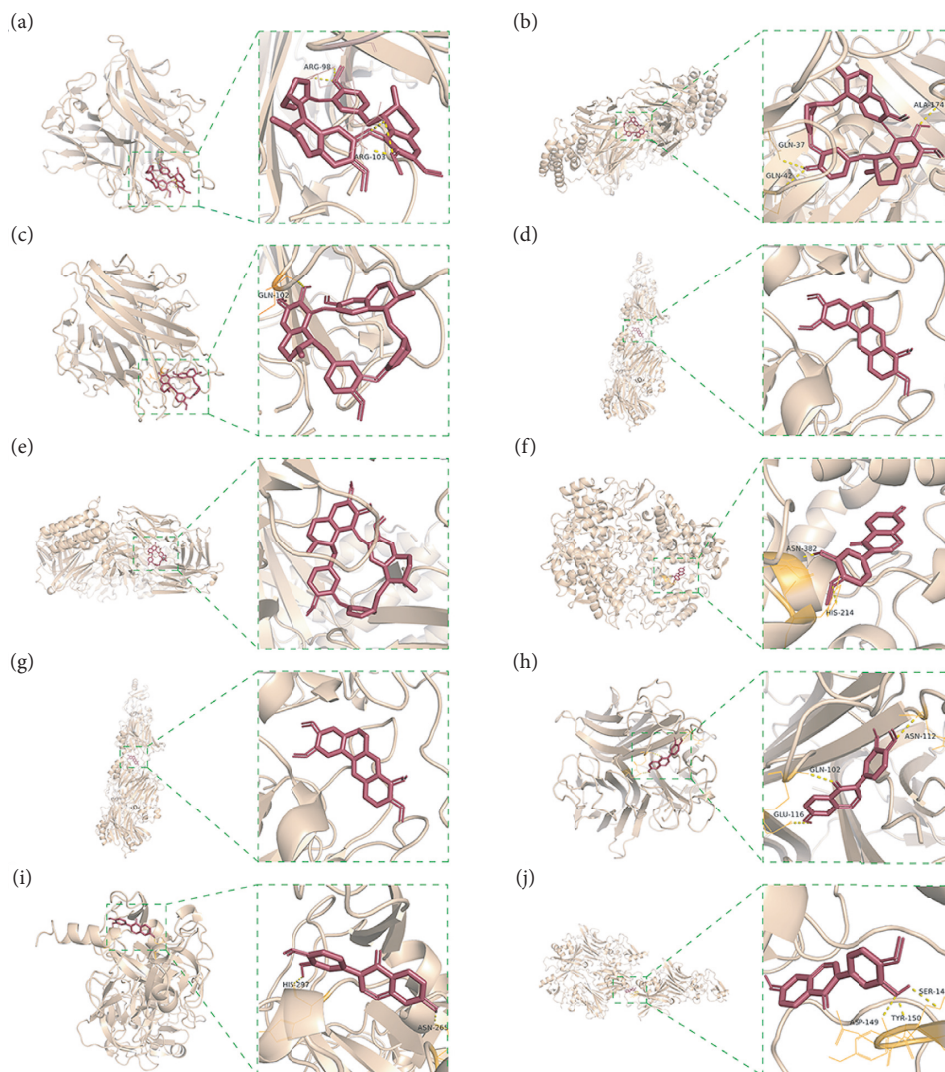
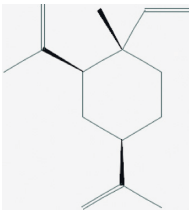
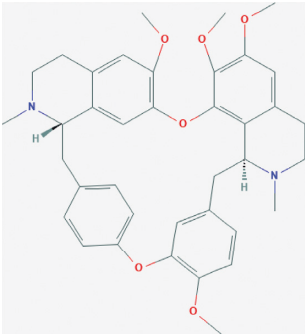
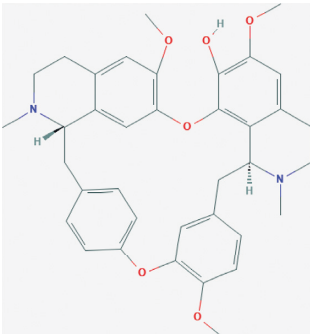
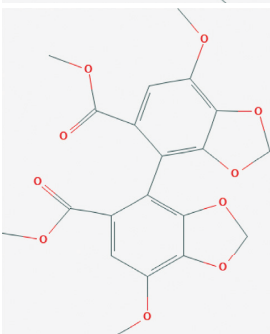
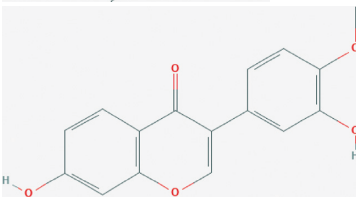
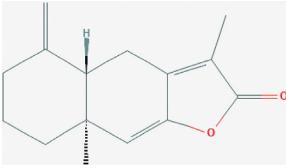
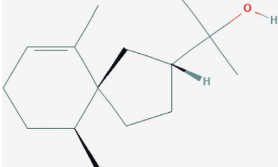


FIGURE 6: Molecular docking of bioactive compounds and hub targets for FHD treating NS. (a) TNF and tetrandrine, affinity =  $-10.1$  kcal/mol. (b) IL10 and fangchinoline, affinity =  $-9.5$  kcal/mol. (c) TNF and fangchinoline, affinity =  $-9.5$  kcal/mol. (d) TNF and palmatine, affinity =  $-8.6$  kcal/mol. (e) IL10 and tetrandrine, affinity =  $-8.6$  kcal/mol. (f) PTGS2 and calycosin, affinity =  $-8.6$  kcal/mol. (g) CCL2 and palmatine, affinity =  $-8.5$  kcal/mol. (h) TNF and calycosin, affinity =  $-8.5$  kcal/mol. (i) TP53 and calycosin, affinity =  $-8.3$  kcal/mol. (j) CCL2 and calycosin, affinity =  $-8.2$  kcal/mol.

TABLE 1: The chemical structure of bioactive compounds from FHD.

Synonyms	Molecular formula	2D structure
Palmatine	$C_{21}H_{22}NO_4^+$	

TABLE 1: Continued.

Synonyms	Molecular formula	2D structure
Beta-elemene	$C_{15}H_{24}$	
Tetrandrine	$C_{38}H_{42}N_2O_6$	
Fangchinoline	$C_{37}H_{40}N_2O_6$	
Bifendate	$C_{20}H_{18}O_{10}$	
Calycosin	$C_{16}H_{12}O_5$	
Atractylenolide I	$C_{15}H_{18}O_2$	
Hinesol	$C_{15}H_{26}O$	

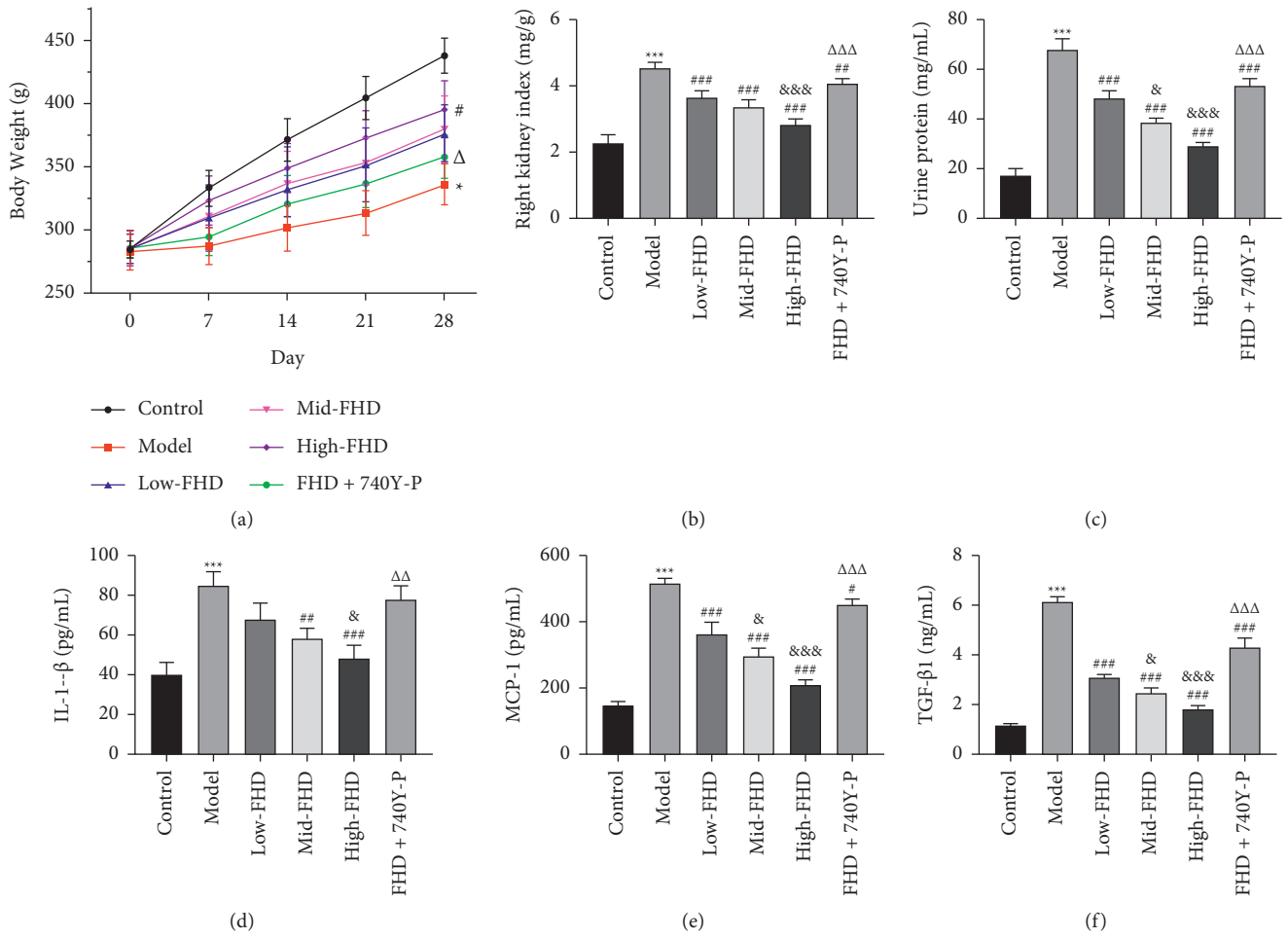


FIGURE 7: Effects of FHD on body weight, kidney weight, proteinuria, and inflammatory response in NS rats via affecting PI3K-Akt signaling pathway. (a) The body weight of rats was recorded once every 4 weeks after treatment. (b) The right kidney index (kidney weight/body weight) of rats. (c) The level of 24 h urine protein in rats was measured using a BCA kit. (d-f) The levels of serum inflammatory factors (IL-1 $\beta$ , MCP-1, and TGF- $\beta$ 1) in rats were measured by the corresponding enzyme-linked immunosorbent assay kits. NS model rats were induced by adriamycin (ADR) and then treated with low- (1 g/kg/d), mid- (2 g/kg/d), high-dose (4 g/kg/d) FHD or/and 740Y-P (a PI3K activator). \*\*\* $P$  < 0.001 compared with the control group; ## $P$  < 0.01 and ### $P$  < 0.001 compared with the model group; & $P$  < 0.05 and &&& $P$  < 0.001 compared with the low-FHD group; and ΔΔ $P$  < 0.01 and ΔΔΔ $P$  < 0.001 compared with the FHD + 740Y-P group.

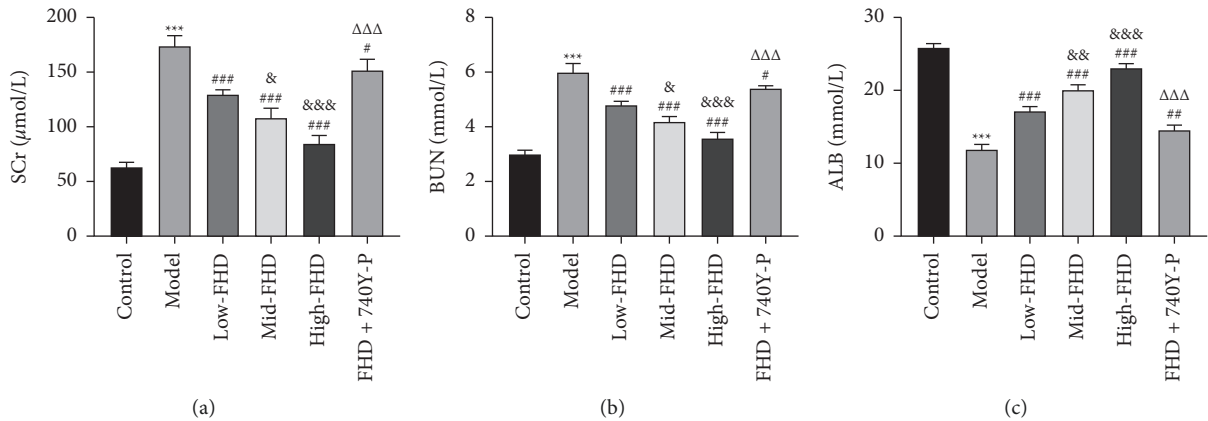


FIGURE 8: Continued.

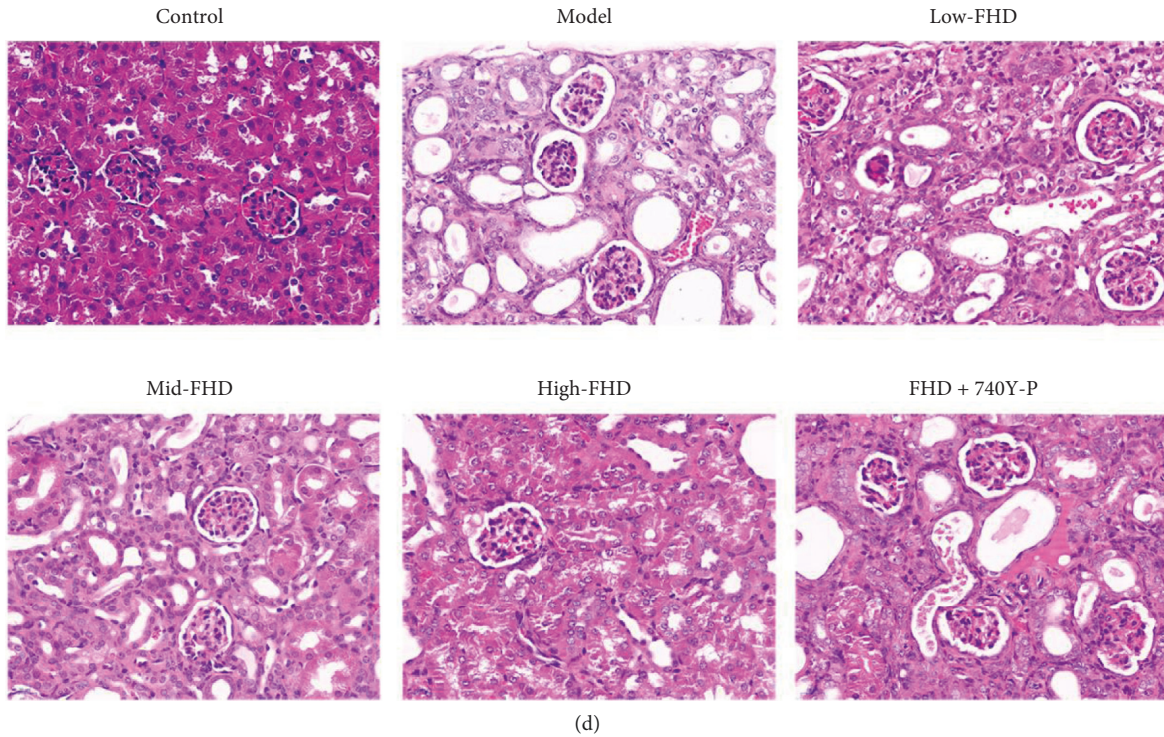


FIGURE 8: Effects of FHD on renal function and histopathology in NS rats via affecting PI3K-Akt signaling pathway. (a–c) The serum levels of renal function indicators (SCr, BUN, and ALB) were detected using a chemical analyzer. (d) Histopathological changes were measured using the hematoxylin and eosin staining. Scale bar = 20  $\mu$ m. NS model rats were induced by ADR and then treated with low-, mid-, and high-dose FHD or/and 740Y-P. \*\*\*  $P < 0.001$  compared with the control group; \*\*  $P < 0.01$  and \*\*\*  $P < 0.001$  compared with the model group; &  $P < 0.05$ , &&  $P < 0.01$ , and &&&  $P < 0.001$  compared with the low-FHD group; and  $\Delta\Delta\Delta P < 0.001$  compared with the FHD + 740Y-P group.

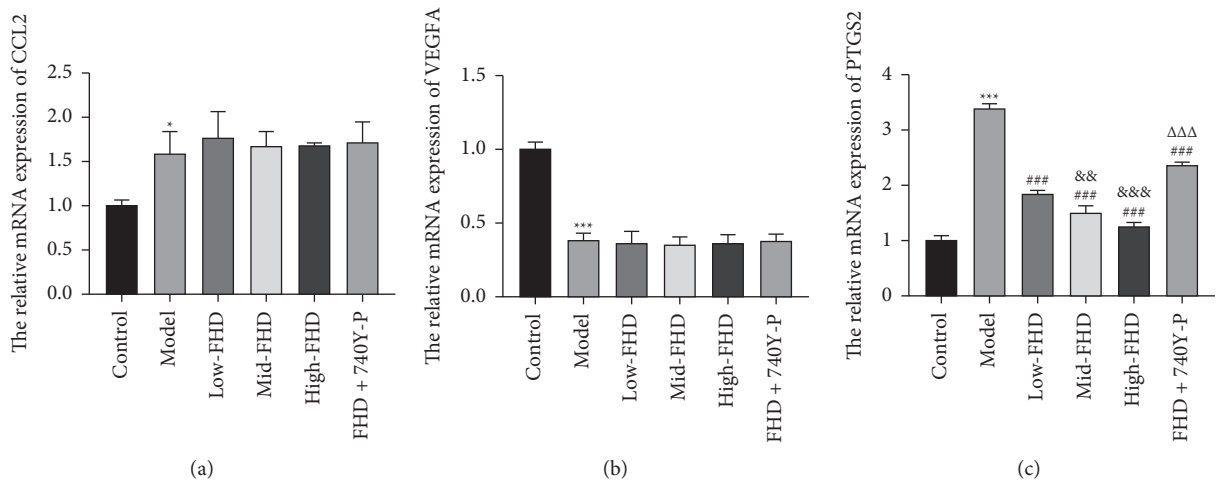


FIGURE 9: Continued.

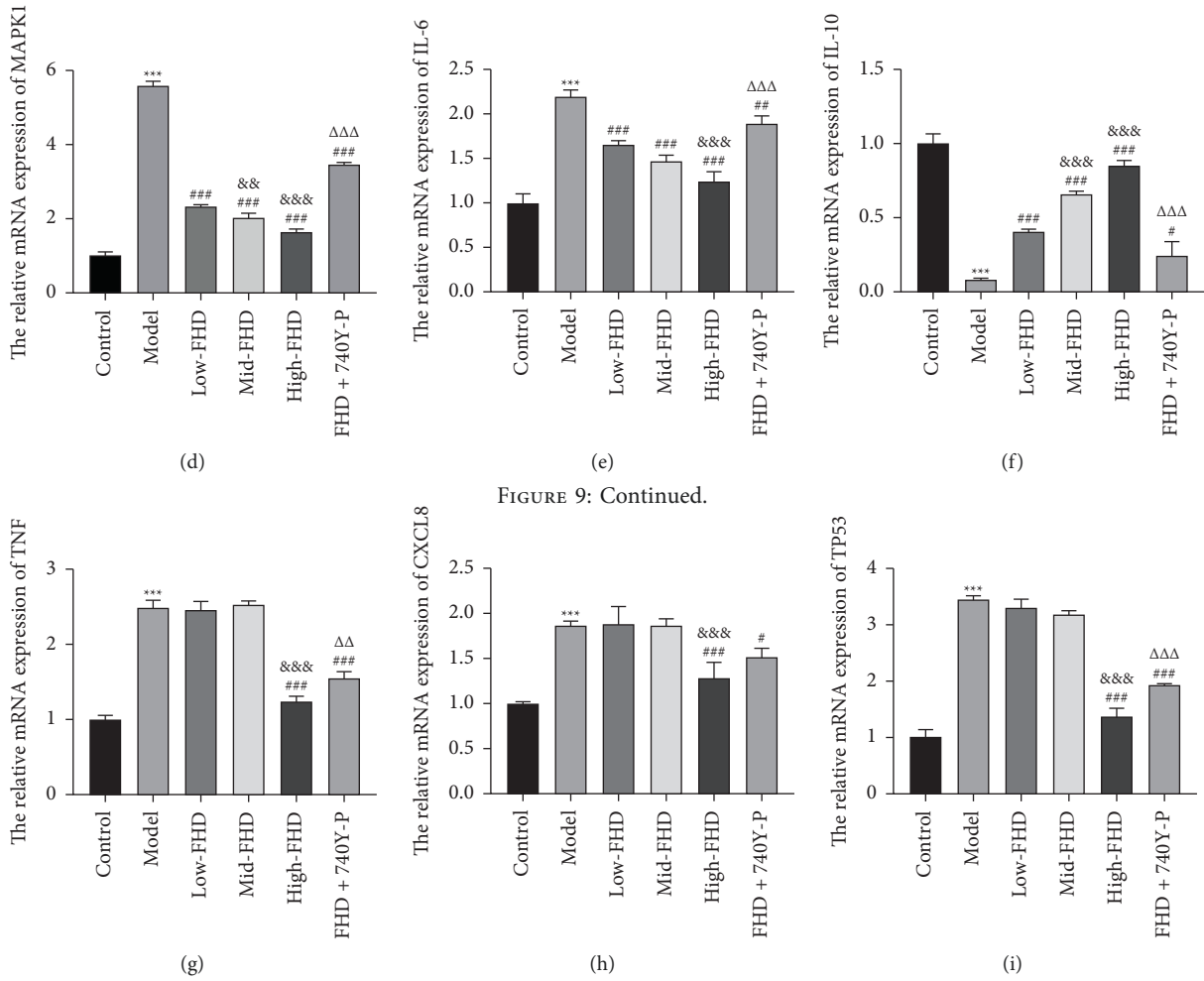


FIGURE 9: Validation of hub targets for FHD against NS by qRT-PCR. (a-i) The relative mRNA expression of CCL2, VEGFA, PTGS2, MAPK1, IL-6, IL-10, TNF, CXCL8, and TP53. NS model rats were induced by ADR and then treated with low-, mid-, and high-dose FHD or/and 740Y-P. \* $P < 0.05$  and \*\*\* $P < 0.001$  compared with the control group; # $P < 0.05$ , ## $P < 0.01$ , and ### $P < 0.001$  compared with the model group; & $P < 0.05$  and && $P < 0.001$  compared with the low-FHD group;  $P < 0.01$  and <sup>ΔΔΔ</sup> $P < 0.001$  compared with the FHD + 740Y-P group.

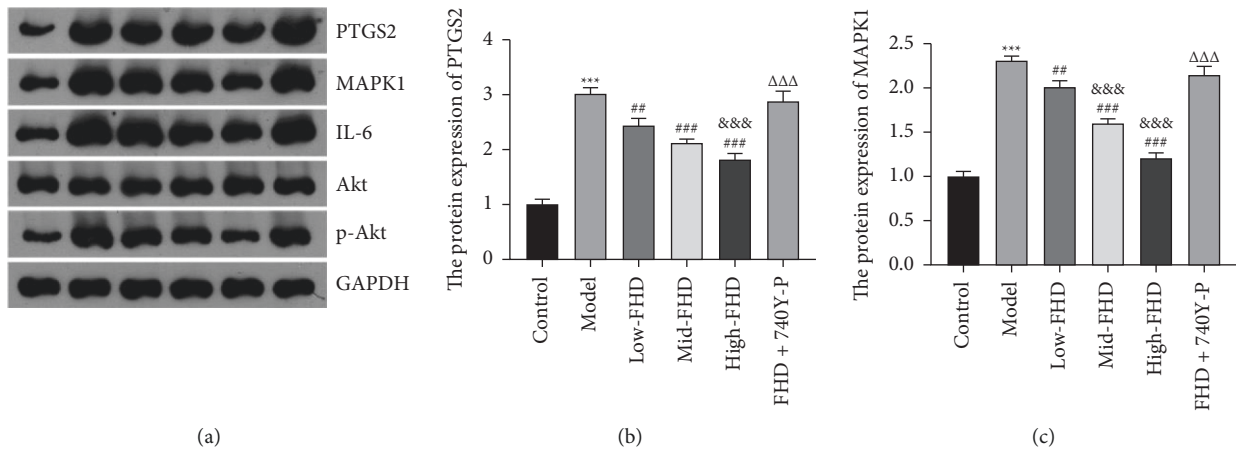


FIGURE 10: Continued.

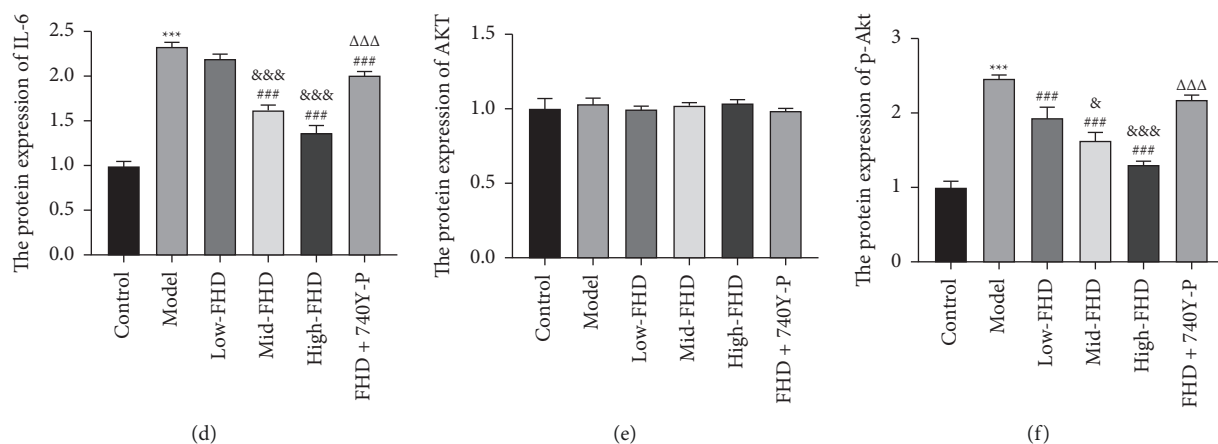


FIGURE 10: Effects of FHD on the expression of PTGS2, MAPK1, IL-6, and PI3K-Akt pathway in NS rats. (a–f) The relative protein expression of PTGS2, MAPK1, IL-6, Akt, and p-Akt was measured by Western blotting. NS model rats were induced by ADR and then treated low-, mid-, and high-dose FHD or/and 740Y-P. \*\*\* $P < 0.001$  compared with the control group; ## $P < 0.01$  and ### $P < 0.001$  compared with the model group; & $P < 0.05$  and && $P < 0.001$  compared with the low-FHD group; and  $\Delta\Delta\Delta P < 0.001$  compared with the FHD + 740Y-P group.

## 5. Conclusion

In summary, network pharmacology predicted that the potential molecular mechanisms of FHD against NS were mainly involved in 9 hub targets and PI3K-Akt signaling pathway. In vivo experiments confirmed the therapeutic effect of FHD on NS and revealed that the underlying mechanisms are closely associated with PI3K-Akt pathway, PTGS2, MAPK1, and IL-6. However, the pharmacological and molecular mechanisms of FHD against NS are needed to be investigated more in depth. This study provides a potential renoprotective drug for NS treatment and offers the important foundation for mechanism investigation.

## Data Availability

The raw data used to support the findings of this study are available from the corresponding author upon request.

## Conflicts of Interest

The authors declare that there are no conflicts of interest regarding the publication of this paper.

## Acknowledgments

This work was supported by Zhejiang Province Welfare Technology Applied Research Project (Grant no. LGF19H290006) and Hangzhou Agricultural and Social Development Research Project (Grant no. 2019120B136).

## Supplementary Materials

Table S1. Primer sequences used in qRT-PCR. Table S2. A total of 114 bioactive compounds of Fangji Huangqi decoction. Table S3. The results of GO enrichment analysis (Top 30). Table S4. The results of KEGG enrichment analysis

(Top 20). Table S5. Molecular docking of bioactive compounds and hub targets. (Supplementary Materials)

## References

- [1] S. A. Politano, G. B. Colbert, and N. Hamiduzzaman, "Nephrotic syndrome," *Primary Care: Clinics in Office Practice*, vol. 47, no. 4, pp. 597–613, 2020.
- [2] C.-s. Wang and L. A. Greenbaum, "Nephrotic syndrome," *Pediatric Clinics of North America*, vol. 66, no. 1, pp. 73–85, 2019.
- [3] M. L. Downie, C. Gallibois, R. S. Parekh, and D. G. Noone, "Nephrotic syndrome in infants and children: pathophysiology and management," *Paediatrics and International Child Health*, vol. 37, no. 4, pp. 248–258, 2017.
- [4] W.-n. Zhang, L. Yang, S.-s. He, A.-p. Li, and X.-m. Qin, "Mechanisms of Chinese medical formula Fangji Huangqi decoction as an effective treatment of nephrotic syndrome based on systems pharmacology," *Chinese Herbal Medicines*, vol. 11, no. 3, pp. 281–291, 2019.
- [5] Y. Guo, B. Chen, X. Pei, and D. Zhang, "Radix stephaniae tetrandrine: an emerging role for management of breast cancer," *Current Pharmaceutical Design*, vol. 26, no. 1, pp. 25–36, 2020.
- [6] Z. Chen, L. Liu, C. Gao et al., "Astragali radix (huangqi): a promising edible immunomodulatory herbal medicine," *Journal of Ethnopharmacology*, vol. 258, Article ID 112895, 2020.
- [7] Y.-J. Kwon, D.-H. Son, T.-H. Chung, and Y.-J. Lee, "A review of the pharmacological efficacy and safety of licorice root from corroborative clinical trial findings," *Journal of Medicinal Food*, vol. 23, no. 1, pp. 12–20, 2020.
- [8] L. Ruqiao, C. Yueli, Z. Xuelan et al., "Rhizoma atractylodis macrocephalae: a review of photochemistry, pharmacokinetics and pharmacology," *Die Pharmazie*, vol. 75, pp. 42–55, 2020.
- [9] J. Liu, A. R. Sternberg, S. Ghiasvand, and Y. Berdichevsky, "Epilepsy-on-a-chip system for antiepileptic drug discovery," *IEEE Transactions on Biomedical Engineering*, vol. 66, no. 5, pp. 1231–1241, 2019.

- [10] R. Zhang, X. Zhu, H. Bai, and K. Ning, "Network pharmacology databases for traditional Chinese medicine: review and assessment," *Frontiers in Pharmacology*, vol. 10, p. 123, 2019.
- [11] R. Varghese and A. Majumdar, "A new prospect for the treatment of nephrotic syndrome based on network pharmacology analysis," *Current Research in Physiology*, vol. 5, pp. 36–47, 2022.
- [12] D. Feng, X. R. Li, Z. Y. Wang et al., "Integrated UPLC-MS and network pharmacology approach to explore the active components and the potential mechanism of Yiqi Huoxue decoction for treating nephrotic syndrome," *Frontiers in Pharmacology*, vol. 12, Article ID 775745, 2022.
- [13] Y. Duan, D. Zhang, Y. Ye et al., "Integrated metabolomics and network pharmacology to establish the action mechanism of qingrekaesen granule for treating nephrotic syndrome," *Frontiers in Pharmacology*, vol. 12, Article ID 765563, 2021.
- [14] W.-N. Zhang, L. Yang, S.-S. He, X.-M. Qin, and A.-P. Li, "Metabolomics coupled with integrative pharmacology reveal the protective effect of Fangjihuangqi decoction against adriamycin-induced rat nephropathy model," *Journal of Pharmaceutical and Biomedical Analysis*, vol. 174, pp. 525–533, 2019.
- [15] Y. Assenov, F. Ramírez, S.-E. Schelhorn, T. Lengauer, and M. Albrecht, "Computing topological parameters of biological networks," *Bioinformatics*, vol. 24, no. 2, pp. 282–284, 2008.
- [16] N. T. Doncheva, J. H. Morris, J. Gorodkin, and L. J. Jensen, "Cytoscape stringapp: network analysis and visualization of proteomics data," *Journal of Proteome Research*, vol. 18, no. 2, pp. 623–632, 2019.
- [17] M. Rebhan, V. Chalifa-Caspi, J. Prilusky, and D. Lancet, "Genecards: integrating information about genes, proteins and diseases," *Trends in Genetics*, vol. 13, no. 4, p. 163, 1997.
- [18] J. Piñero, J. M. Ramírez-Anguita, J. Saüch-Pitarch et al., "The disgenet knowledge platform for disease genomics: 2019 update," *Nucleic Acids Research*, vol. 48, pp. 845–855, 2020.
- [19] D. Szklarczyk, A. Franceschini, M. Kuhn et al., "The string database in 2011: functional interaction networks of proteins, globally integrated and scored," *Nucleic Acids Research*, vol. 39, pp. D561–D568, 2011.
- [20] H. Mi, A. Muruganujan, and P. D. Thomas, "Panther in 2013: modeling the evolution of gene function, and other gene attributes, in the context of phylogenetic trees," *Nucleic Acids Research*, vol. 41, pp. D377–D386, 2013.
- [21] T. Sterling and J. J. Irwin, "Zinc 15 - ligand discovery for everyone," *Journal of Chemical Information and Modeling*, vol. 55, no. 11, pp. 2324–2337, 2015.
- [22] G. M. Morris, R. Huey, W. Lindstrom et al., "Autodock4 and autodocktools4: automated docking with selective receptor flexibility," *Journal of Computational Chemistry*, vol. 30, no. 16, pp. 2785–2791, 2009.
- [23] D. S. Goodsell, C. Zardocki, L. Di Costanzo et al., "RCSB protein data bank: enabling biomedical research and drug discovery," *Protein Science*, vol. 29, no. 1, pp. 52–65, 2020.
- [24] D. Seeliger and B. L. de Groot, "Ligand docking and binding site analysis with pymol and autodock/vina," *Journal of Computer-Aided Molecular Design*, vol. 24, no. 5, pp. 417–422, 2010.
- [25] O. Trott and A. J. Olson, "Autodock vina: improving the speed and accuracy of docking with a new scoring function, efficient optimization, and multithreading," *Journal of Computational Chemistry*, vol. 31, pp. 455–461, 2010.
- [26] L. Tan, Y. Tu, K. Wang, B. Han, H. Peng, and C. He, "Exploring protective effect of glycine tabacina aqueous extract against nephrotic syndrome by network pharmacology and experimental verification," *Chinese Medicine*, vol. 15, no. 1, p. 79, 2020.
- [27] H. Zhang, R. Zhang, J. Chen, M. Shi, W. Li, and X. Zhang, "Exploring protective effect of glycine tabacina aqueous extract against nephrotic syndrome by network pharmacology and experimental verification," *Kidney & Blood Pressure Research*, vol. 42, no. 5, pp. 894–904, 2017.
- [28] Q. Di Tu, J. Jin, X. Hu, Y. Ren, L. Zhao, and Q. He, "Curcumin improves the renal autophagy in rat experimental membranous nephropathy via regulating the pi3k/akt/mTOR and nrf2/ho-1 signaling pathways," *BioMed Research International*, vol. 2020, Article ID 7069052, 12 pages, 2020.
- [29] J. Yin, J. Lin, J. Yu, X. Wei, B. Zhu, and C. Zhu, "Tetrandrine may treat membranous glomerulopathy via p13k/akt signaling pathway regulation: therapeutic mechanism validation using heyman nephritis rat model," *Bioengineered*, vol. 12, no. 1, pp. 6499–6515, 2021.
- [30] G. Liu and L. He, "Salidroside attenuates adriamycin-induced focal segmental glomerulosclerosis by inhibiting the hypoxia-inducible factor-1 $\alpha$  expression through phosphatidylinositol 3-kinase/protein kinase B pathway," *Nephron*, vol. 142, no. 3, pp. 243–252, 2019.
- [31] C. Xia, L. Shao, Y. Ma et al., "Protective action of ultrasound-guided intraparenchymal transplantation of BMSCs in adriamycin nephropathy rats through the ripk3/mlkl and nlrp3 pathways," *Acta Histochemica*, vol. 123, no. 7, p. 151773, 2021.
- [32] H. Yao, Z. Y. Cai, and Z. X. Sheng, "Nac attenuates adriamycin-induced nephrotic syndrome in rats through regulating tlr4 signaling pathway," *European Review for Medical and Pharmacological Sciences*, vol. 21, pp. 1938–1943, 2017.
- [33] B. Ding, G. Ma, Z. Wang, W. Liang, and W. Gao, "Mechanisms of kidney cell pyroptosis in chronic kidney disease and the effects of traditional Chinese medicine," *Evidence-based Complementary and Alternative Medicine*, vol. 2021, Article ID 1173324, 10 pages, 2021.
- [34] N. A. Maksimowski, J. W. Scholey, and V. R. Williams, "Sex and kidney ace2 expression in primary focal segmental glomerulosclerosis: a neptune study," *PLoS One*, vol. 16, no. 6, Article ID e0252758, 2021.
- [35] M. Xiao, S. Bai, J. Chen et al., "Correlation of TNF- $\alpha$  and IL-10 gene polymorphisms with primary nephrotic syndrome," *Experimental and Therapeutic Medicine*, vol. 20, p. 87, 2020.
- [36] S. He, A. Li, W. Zhang et al., "An integrated transcriptomics and network pharmacology approach to exploring the mechanism of adriamycin-induced kidney injury," *Chemico-Biological Interactions*, vol. 325, Article ID 109096, 2020.
- [37] A. Al-Eisa, M. Al Rushood, and R. Al-Attayah, "Urinary excretion of IL-1 $\beta$ , IL-6 and IL-8 cytokines during relapse and remission of idiopathic nephrotic syndrome," *Journal of Inflammation Research*, vol. 10, pp. 1–5, 2017.
- [38] F.-J. Guan, Q.-Q. Peng, L.-I. Wang, X.-B. Yan, C. Dong, and X.-H. Jiang, "Histone deacetylase-2 expression and activity in children with nephrotic syndrome with different glucocorticoid response," *Pediatric Nephrology*, vol. 33, no. 2, pp. 269–276, 2018.
- [39] X. Nie, M. A. Chanley, R. Pengal, D. B. Thomas, S. Agrawal, and W. E. Smoyer, "Pharmacological and genetic inhibition of downstream targets of p38 MAPK in experimental nephrotic syndrome," *American Journal of Physiology - Renal Physiology*, vol. 314, no. 4, pp. F602–F613, 2018.
- [40] R. J. Motzer, R. Banchereau, H. Hamidi et al., "Molecular subsets in renal cancer determine outcome to checkpoint and



- angiogenesis blockade,” *Cancer Cell*, vol. 38, no. 6, pp. 803–817, 2020.
- [41] K. Tanabe, J. Wada, and Y. Sato, “Targeting angiogenesis and lymphangiogenesis in kidney disease,” *Nature Reviews Nephrology*, vol. 16, no. 5, pp. 289–303, 2020.
- [42] L. Su, P. Cao, and H. Wang, “Tetrandrine mediates renal function and redox homeostasis in a streptozotocin-induced diabetic nephropathy rat model through nrf2/ho-1 reactivation,” *Annals of Translational Medicine*, vol. 8, no. 16, p. 990, 2020.
- [43] Y.-y. Zhang, R.-z. Tan, X.-q. Zhang, Y. Yu, and C. Yu, “Calycosin ameliorates diabetes-induced renal inflammation via the NF- $\kappa$ B pathway in vitro and in vivo,” *Medical Science Monitor*, vol. 25, pp. 1671–1678, 2019.
- [44] Y. Jiang, J. Liu, Z. Zhou, K. Liu, and C. Liu, “Fangchinoline protects against renal injury in diabetic nephropathy by modulating the mapk signaling pathway,” *Experimental and Clinical Endocrinology & Diabetes*, vol. 128, no. 8, pp. 499–505, 2020.
- [45] X. Peng, Y. Wang, H. Li et al., “ATG5-mediated autophagy suppresses NF- $\kappa$ B signaling to limit epithelial inflammatory response to kidney injury,” *Cell Death & Disease*, vol. 10, no. 4, p. 253, 2019.